CREATION OF HAZARD MAPS BY CONSIDERING REGIONAL CHARACTERISTICS BY MICROTREMORS

Tsutomu OCHIAI[1], Tetsushi INUBUSHI[2] and Takahisa ENOMOTO[3]

[1] Member, Research Associate, Dept. of Arch. and Building Eng., Kanagawa University,
Kanagawa, Japan, ochiai@kanagawa-u.ac.jp
[2] Member, Senior Lecturer, Faculty of Architecture, Kindai University,
Osaka, Japan, inubushi@arch.kindai.ac.jp
[3] Member, Professor, Dept. of Arch. and Building Eng., Kanagawa University,
Kanagawa, Japan, enomot01@kanagawa-u.ac.jp

ABSTRACT: The aim of this study is to understand the ground hazards of an area by considering its ground-vibration characteristics by means of a relatively simple method based on the horizontal-to-vertical spectral ratio (HVSR) derived using single-point microtremor observations. The applicability of evaluating the ground hazard as the product of the predominant period and peak value from the HVSR is examined. It is confirmed that the ground-hazard distribution map so created is consistent with the average shear-wave velocity in the upper 30 m, which is a seismic-code standard.

Keywords: Microtremor, H/V spectral ratio (HVSR), Hazard map, Yokohama City, Kanagawa Prefecture

1. INTRODUCTION

In Japan, earthquake damage has generally been estimated at prefecture level, but recent years have seen expectations of detailed damage estimations at municipal level. The many past seismic-wave damage surveys make it apparent that building damage differs depending on the structural characteristics of the underlying ground. In particular, the Japanese city of Yokohama (hereinafter referred to simply as Yokohama), which is the focus of the present study, has a record of the 1923 Great Kanto Earthquake. Predicting damage in detail requires data on the vibration characteristics of the ground surface, and various methods have been tried to acquire such data, including borehole surveys and earthquake data records. However, a particularly effective way to obtain ground-vibration characteristics over a wide area is to use microtremor (MT) observations.

Various studies have provided a logical interpretation of the horizontal-to-vertical spectral ratio (HVSR) based on MTs, noting that MTs are affected by the underground structure near the observation points. For example, Nakamura[1] interpreted the HVSR as the amplification rate in relation to the ground, whereas Tokimatsu and Tamura[2] interpreted it as the fundamental mode in relation to Rayleigh waves. Furthermore, others have investigated the use of diffuse-waveform theory based on the assumption that the MT-vibration source is distributed uniformly[3]. Several other studies have

focused on HVSR stability. Compared to a simple horizontal spectrum, the HVSR stabilizes regardless of the measurement time, and the peak-cycle disparity is approximately 5%[4]. Some recent studies have evaluated the risk in terms of that of ground shaking based on the MT HVSR[5].

Since the 1990s, we have been making high-density MT observations, mainly in the Japanese prefecture of Kanagawa (hereinafter referred to simply as Kanagawa)[6, 7]. We used both the predominant period (horizontal axis, Tm) and peak value (vertical axis, Rm) from the HVSR in Yokohama and investigated the applicability of defining ground hazard (GH) as a simple ground-evaluation indicator.

2. TERRAIN AND GEOLOGY OF YOKOHAMA

A map of the geology[8] overlain on the topography and a microtopographical classification map[9] of Yokohama are shown in Fig. 1. The terrain includes hillocks, plateaus, terraces, lowlands, and landfill. The hillocks and plateaus comprise approximately 70% of the total area of the city, and the remaining 30% comprises alluvial lowlands alongside rivers and landfill in the littoral zone.

The hillocks, which are mainly west of the central area of the city, intersect the city area from north to south. They have different characteristics in the north and south areas surrounding the Katabira River as it flows through Hodogaya-Ku and Asahi-Ku. The hillocks on the north side are toward the south of the Tama Hills, and their heights increase from 60 m to 100 m going northward. The Miura Hills are in the south of the hillocks on the southern side of the city and continue toward the Miura Peninsula with heights increasing from 80 m to 160 m southward.
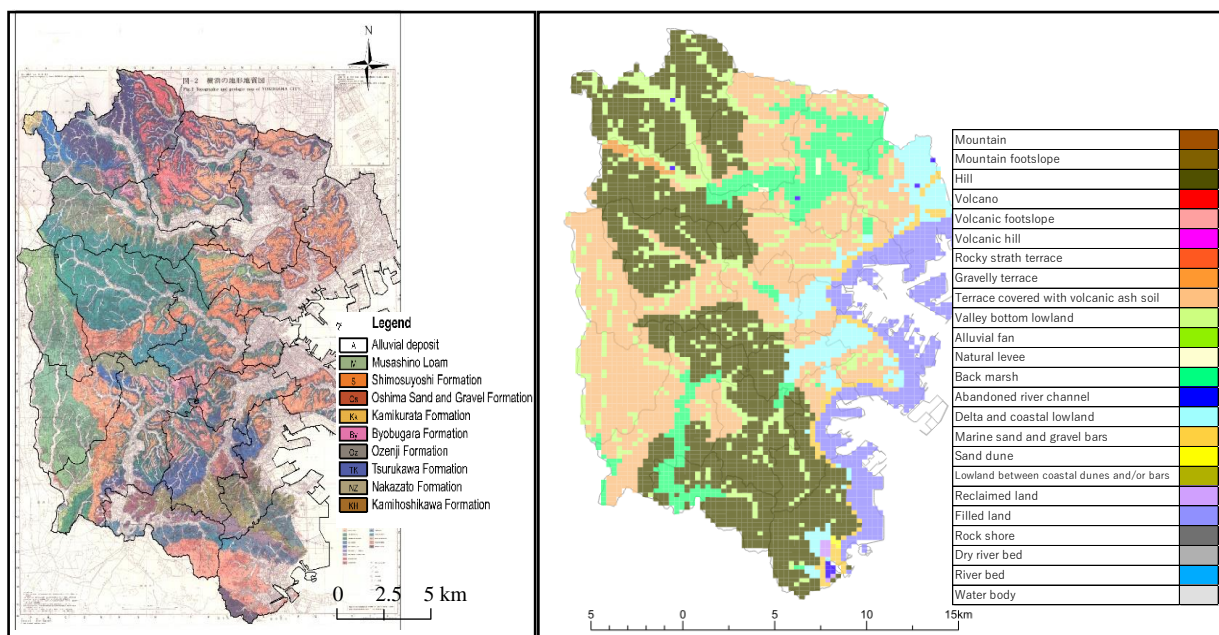

Fig. 1 Yokohama terrain topology and geology (left)[8] and geomorphology (right)[9]

3. MICROTREMOR AND STRONG MOTIN OBSERVATION

3.1 Microtremor observation method

Since the 1990s, we have conducted continuous MT observations, mainly in Kanagawa. In Yokohama, the base was a 250 m × 250 m mesh (a quarter-area mesh)[10], and observations were recorded at approximately 5700 points with the observation point near the center of mesh. The distribution of observation points in Yokohama, including those at which strong motion (SM) has been observed, is shown in Fig. 2. Each recorded observation includes three elements of topographical data, namely two in the horizontal direction (EW and NS) and one in the vertical direction (UD). The recording sampling frequency was 100 Hz and the observation time was 180 s. Also recorded were the map- and GPS-based positional information (latitude/longitude) and the observation conditions. For long-term observation, we use several types of observation equipment (see Table 1) based on the observation period. However, we also perform huddle tests—as necessary—between equipment installations, and these confirm that any equipment-based differences are within the scope of this study's target frequency band (0.5–10 Hz) (0.1–2.0 s).
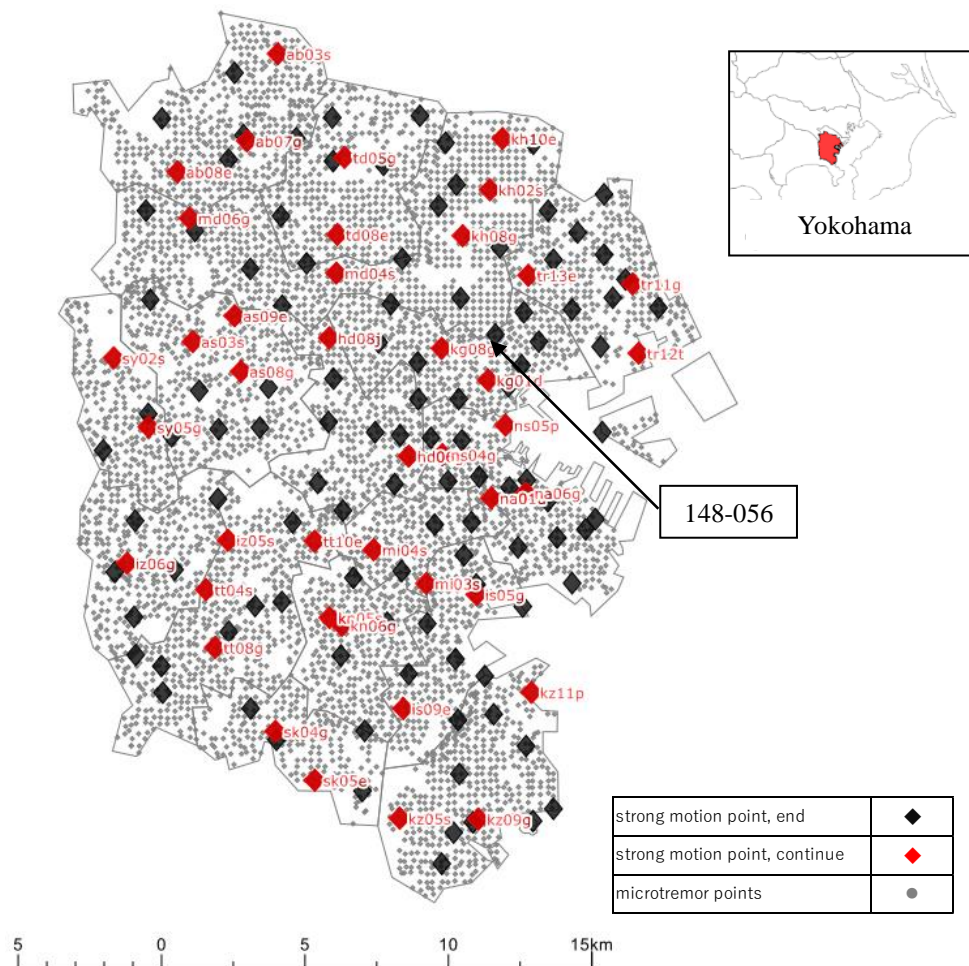

Fig. 2 Microtremor (MT) observation points (gray dots) and strong-motion (SM) observation points (black and red diamonds)

Table 1 Observation equipment used (C, D, and E for Yokohama observations)

	A	B	C	D	E
Recoder	DR-F2a TEAC	UPS-T3 Shindo Giken	SPC-35 Tokyo Sokushin	SPC-51 Tokyo Sokushin	JU410 Hakusan kougyou (Recorders, amplifiers, One sensor)
Amp	AL-120-F Tokyo Sokushin				
Sensor	QST_111 QST_112 Tokyo Sokushin Velocity sensor Natural frequency : 1.0 Hz	UP-225S Shindo Giken Velocity sensor Frequency characteristic : 0.3-10.0 Hz	VSE-15D Tokyo Sokushin Velocity sensor Frequency characteristic : 0.2-10.0 Hz		Accelerometer Frequency characteristic : 0.2-10.0 Hz

3.2 Microtremor analysis policies and observation results

For each element of the observed waveform data (NS, EW, and UD), a stable 20.48 s section with comparatively little noise was extracted, and its Fourier spectrum was calculated. We used a 0.3 Hz-bandwidth Parzen window to smooth the calculated Fourier spectrum. Furthermore, to calculate the HVSR for each section, this was divided by the horizontal two-element (two-dimensional) spectrum, which was the geometric mean of the two horizontal-component spectra in each section by the upper and lower components. Finally, we calculated the average HVSR for all the extracted sections. Examples of the time-history waveforms and spectra from the observation records are shown in Fig. 3.

In this study, because we generally targeted ground surfaces above engineering ground, within approximately 0.1–2.0 s of the cycle, dominant cycles and peak values could be read from particularly prominent HVSR peak values. The dominant cycle for the MT HVSR was set to Tm, and the peak value was set to Rm. In principle, to read the peak from the HVSR, clear peak points with a spectrum ratio of 2.0 or above were considered indicative of the dominant cycle. However, in the absence of a visibly clear peak, multiple peak points were considered as candidates and were evaluated by referencing the dominant cycle, borehole data, and the geology of the surrounding terrain.
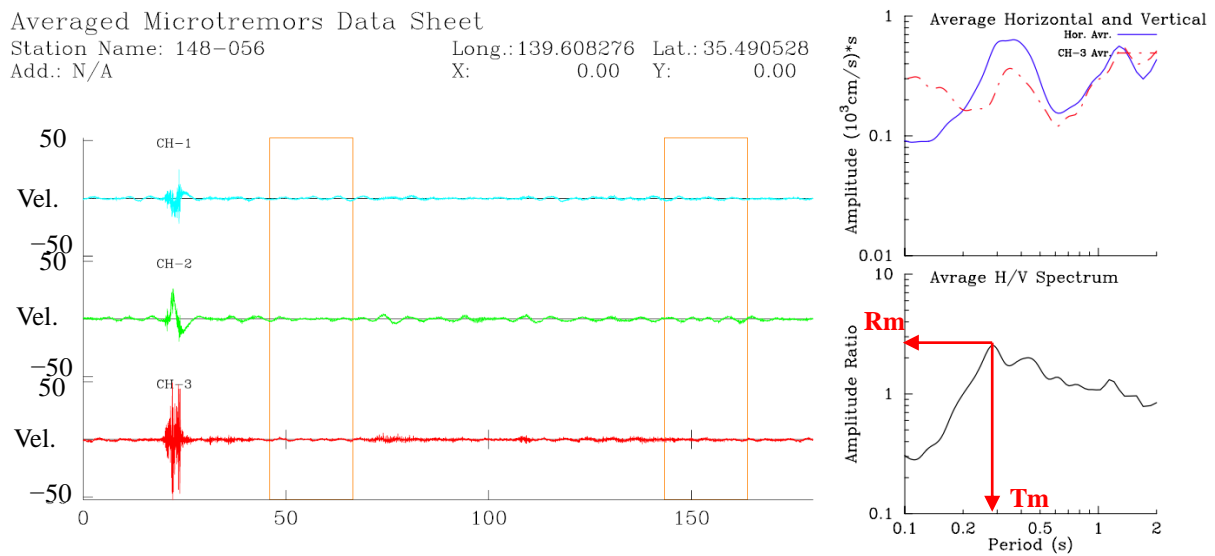

Fig. 3 Example of MT observation results (No. 148-056)

3.3 Microtremor observation and strong-motion observation records

The municipality of Yokohama currently collects and publishes online the records of its SM seismograph network[11]. Toshinawa et al.[12] also published observational records of SM and MTs in Yokohama. A positive correlation has been confirmed by authors between their MT SM spectrum ratio, which was based on bedrock, and the SM record spectrum ratio HVSR defined herein. Using the SM records of 2002–2004 (150 points from eight earthquakes), we performed a comparative analysis of MTs and SM[13]. For this study, we performed the same investigation using the SM records from recent years (2012–2018) (42 points from continuous observation; five earthquakes). Referring to past investigations to guide our selection, we chose observational records of tremors from 277 earthquakes during the target period based on the following criteria: (i) the earthquake magnitude was relatively large (M = 4.5 or greater); (ii) the seismic source depth of the earthquake was at least 30 km (assumed to be vertical at all points); (iii) observation records could be obtained at 90% (37) of all observation points. Table 2 lists the SM observation records, and Fig. 4 shows the seismicity distribution including past investigations.

The SM observation records were organized with a focus on two coda sections that are considered to be the main tremors (60 s from the start of observation) and the increasing surface-wave elements. These coda sections were obtained by constructing a cumulative curve from the absolute amplitude values from the time-history waveforms; 20.48 s were eliminated from the section subsequent to the cumulative value reaching 80%, and the spectrum was obtained using Fourier analysis. The analysis involved smoothing with a 0.3-Hz-bandwidth Parzen window synchronous with the tremor record, and the HVSR was obtained by dividing the horizontal two-element geometric mean by the vertical elements (Fig. 5); in the SM record (coda section) are shown the dominant cycle (T_s) and peak value (R_s).

With reference to the SM observation records (sections that include main tremors or codas) at the target points (42 locations) and nearby MT HVSR (Figs. 6 and 7), we used the subsurface geologic structure based on a borehole survey from compressional and shear (PS) logging for each target point. We also derived the surface-arrival function (line form) for the input motion obtained using S-wave multiple-reflection theory. The SM observation records generally exhibited the same trends as those of the sections, including the main tremors and coda spectra. Excluding where the peaks were virtually unrecognizable with HVSR, the SM records and MT-dominant cycles were approximately the same in at least 70% of the total (inverted triangle in Figs. 6 and 7), and the transfer function also exhibited the same trends. However, as observed in the past investigations, although a certain degree of relationship could be seen for peak values, a clear correlation could not be seen to the same extent as with the dominant cycle. One reason why the dominant cycles from the respective results appear to be nearly matched is that the contrast between the engineering ground and the ground surface for the target region is relatively clear; however, we plan to investigate further adjustments, such as increasing the number of seismic motions that we evaluate.

The plots from past investigations[13] and the current plot are seen to overlap in Fig. 8, along with the corresponding regression curves (straight lines) and correlation coefficients. The dominant cycles for MT and SM records (codas) generally have the same tendencies as those in past investigations, and they match to the extent that the cycles are shorter than 0.5 s. The peak values for MT and SM records (codas) fairly show the same tendencies as those in past investigations. The peak values were mostly the same low values (< 3), and if they exceeded this, we confirmed that the SM records (codas) tended to be larger. We found that the disparity from the whole of the peak values was larger across large cycles and where the peak value was large, apparently because of ground nonlinearity. Furthermore, when compared to past investigations, the correlation coefficient between the dominant cycle and peak value was slightly worse, presumably because there were far fewer target points (42 instead of 150).

Table 2 Observations of strong motion

	No.	Day	Epicenter		Depth	M
			Lat.	Lon.	km	
Past investigations	1-1	2002/2/12 22:44	35.59	141.90	48	5.5
	1-2	2003/5/12 0:57	35.87	140.90	47	5.2
	1-3	2003/5/17 23:33	35.73	140.65	47	5.1
	1-4	2003/5/26 18:24	38.80	141.68	71	7.0
	1-5	2002/9/20 12:55	35.22	140.30	70	5.8
	1-6	2003/10/15 16:30	35.61	140.50	74	5.1
	1-7	2003/10/31 10:06	37.33	142.70	33	6.8
	1-8	2003/11/15 3:44	36.43	141.17	48	5.8

	No.	Day	Epicenter		Depth	M
			Lat.	Lon.	km	
This investigations	2-1	2012/11/24 17:59	35.64	140.20	72	4.8
	2-2	2013/4/14 10:22	36.00	139.50	97	4.6
	2-3	2014/5/5 5:18	34.95	139.48	156	6.0
	2-4	2014/9/16 9:16	36.90	139.86	47	5.6
	2-5	2016/11/23 3:45	34.54	140.07	101	4.5
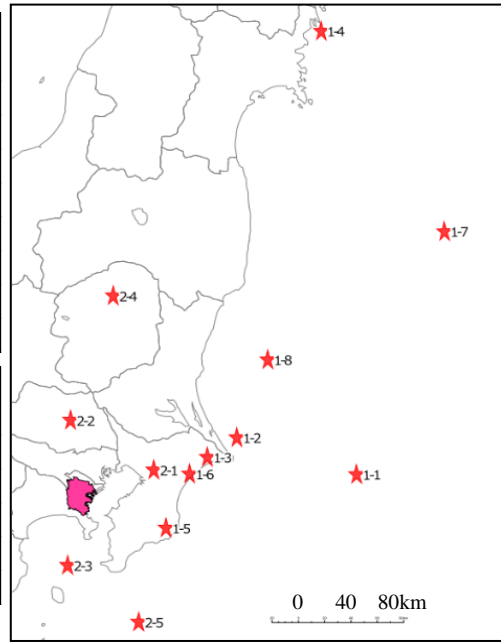
Fig. 4 Seismicity map

Section extracted from time-history waveform (three elements) of SM record.
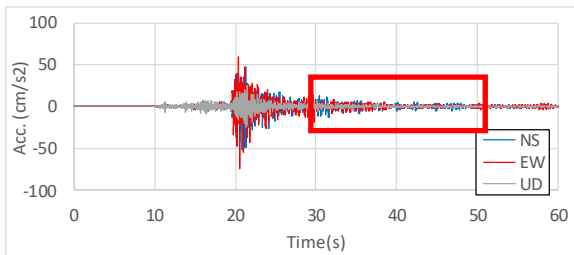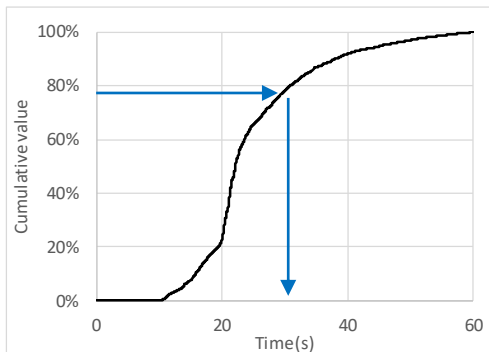
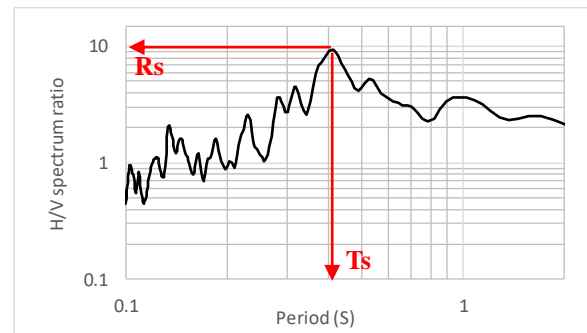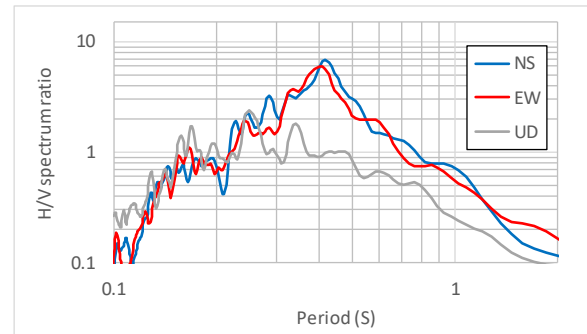**Fourier spectrum (top) and HVSR (bottom)**

Cumulative curve

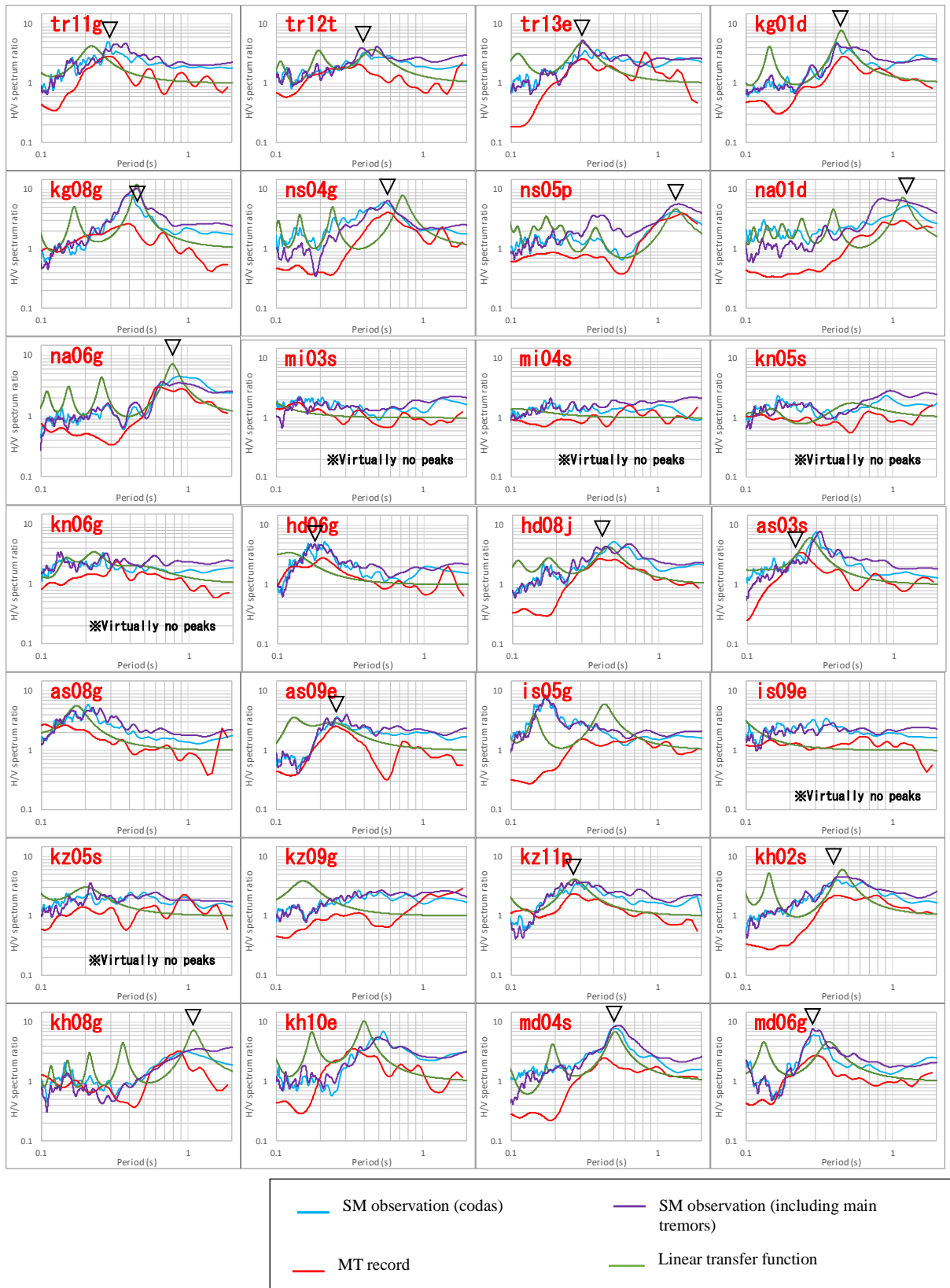Fig. 5 Data organization and flow of SM observation record (coda section)

Fig. 6 SM observations and MT horizontal-to-vertical spectral ratio (HVSR) (1)
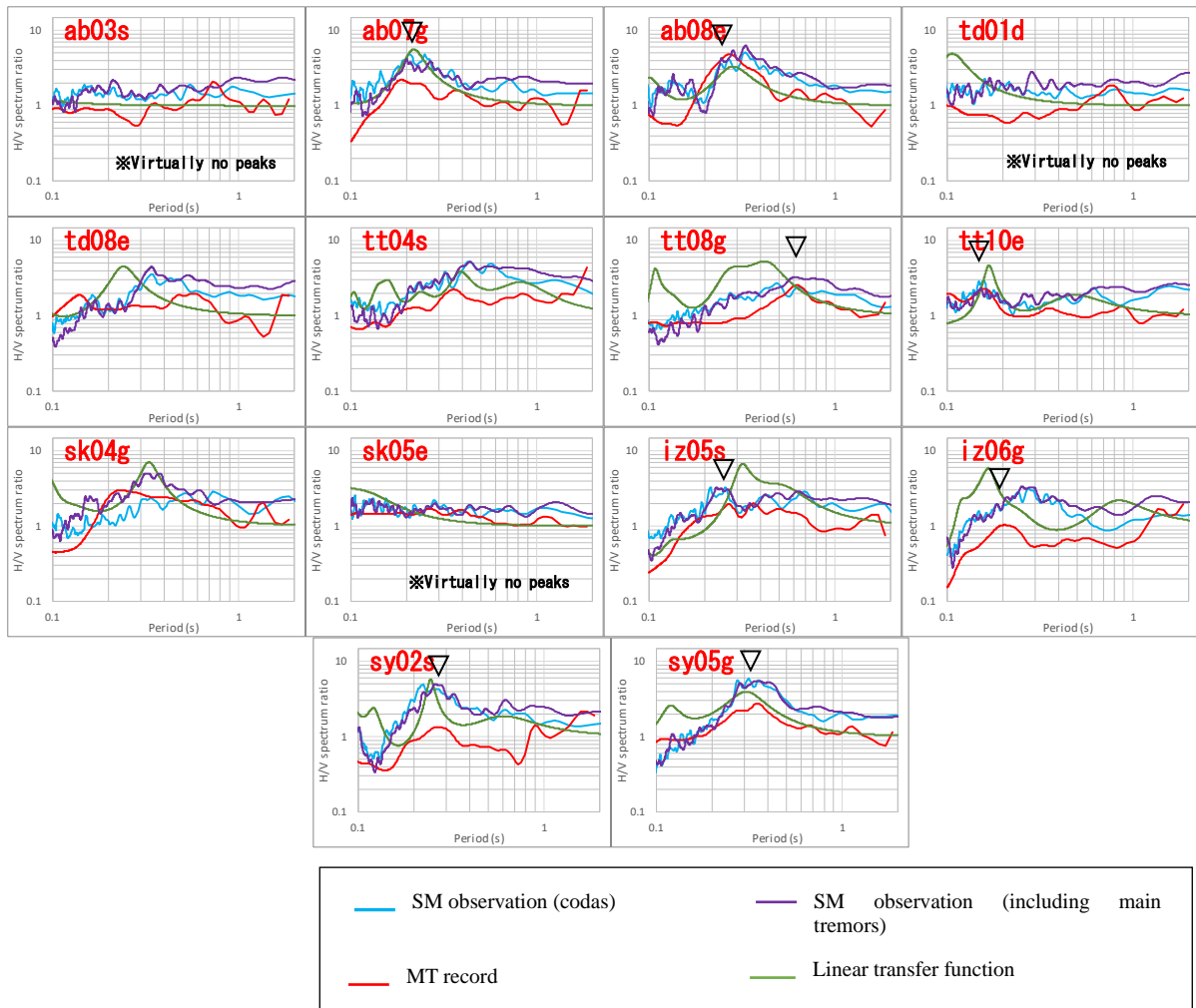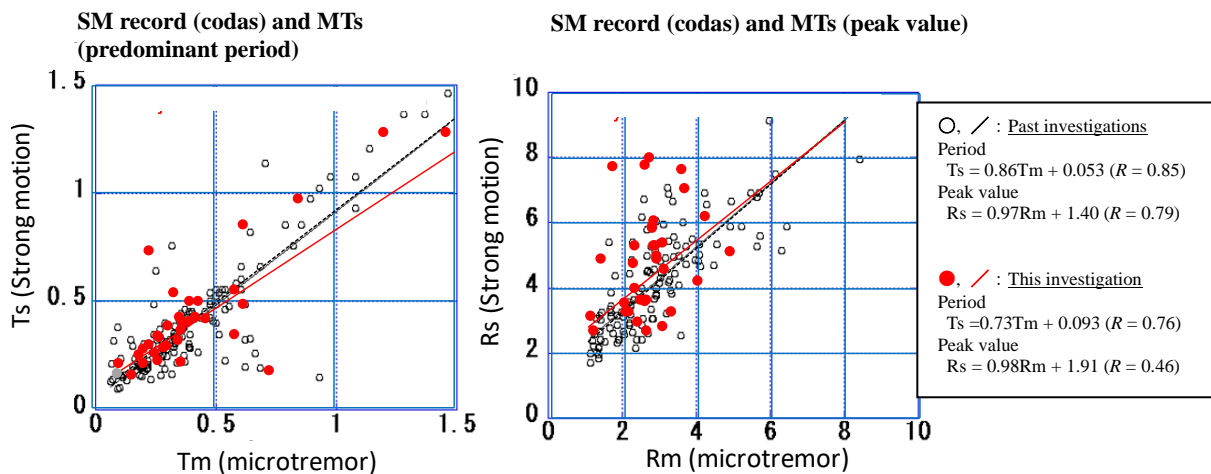
Fig. 7 SM observations and MT HVSR (2)

Fig. 8 Comparison of MT and SM observation records (codas)

4. PREDOMINANT PERIOD AND PEAK-VALUE DISTRIBUTION BASED ON HVSR CHARACTERISTICS

This study was organized using geomorphology. In this section, the levels of Tm and Rm disparity (Fig. 9) are summarized; they are higher for both Tm and Rm in lowland geomorphology (such as back swamps and deltas or coastal lowlands) and reclaimed land.

From the distribution maps (Fig. 10), several such areas were confirmed along rivers wherein the values for both Tm and Rm were large (A). By contrast, there were areas (B) where Tm was not as large, areas (C) where both were of medium size, and areas (D) where both were small.
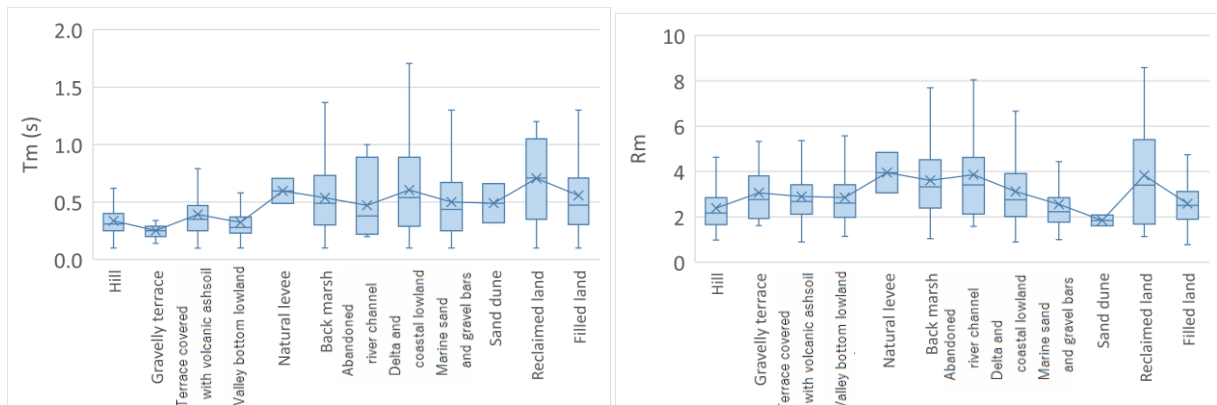

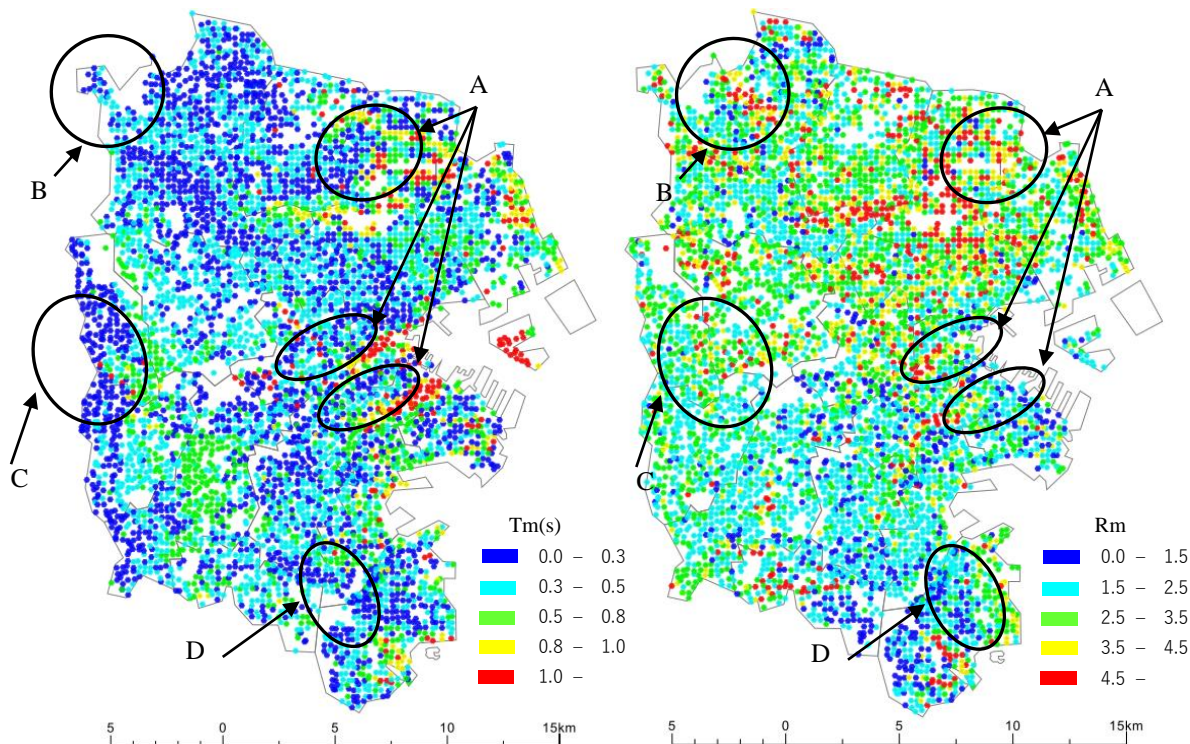Fig. 9 Predominant-period (left) and peak-value (right) disparity by geomorphology

Fig. 10 Predominant-period (Tm) (left) and peak-value (Rm) (right) distributions

5. GROUND-HAZARD EVALUATION BASED ON MICROTREMOR HVSR FEATURES

5.1 Proposed method for evaluating ground hazard

Attempting to create a simple map to use to evaluate GH, we focused on the HVSR predominant period (Tm) and peak value (Rm). When creating a GH map from past earthquakes, it is common to use existing borehole data to create a GH model[14), 15)]. However, because there is regional bias in terms of the number of borehole data, the accuracy of the ground model in areas with limited data is unreliable. Therefore, we used high-density MT observation results to evaluate GH risk uniformly.

Our evaluation generally indicates that the longer the seismic-motion cycle and the greater the amplitude, the greater the impact on structures because of the increased seismic-motion energy. In the target area of this study, for the HVSR obtained from amplification characteristics (including main motion and MTs), we confirmed a strong correlation (Figs. 6–8). Therefore, we defined the GH as an indicator for preliminary evaluation (PE) of the impact of an earthquake on a structure, and this value obtained as PE = Tm × Rm, where PE is the GH, Tm is the predominant period, and Rm is the peak value.

The GH is basically equivalent to the area obtained from the seismic-motion HVSR predominant period and peak value. Therefore, generally, the amount of energy (impact range) applied to a structure can be evaluated in terms of the GH obtained from the MT HVSR. Nakamura et al.[5)] used the MT HVSR dominant cycle and peak amplitude and this method to evaluate the risk of ground sway.

5.2 Ground-hazard distribution and comparison with data from interpretation of past investigations

The level of GH disparity by geomorphology is shown in Fig. 11. For both the Tm and Rm shown in Fig. 9, the disparity was greatest in lowland areas, such as back swamps and deltas/coastal lowlands, and reclaimed land.

Using Tokyo-region risk-judgment[16)] data as the reference, the GH can be given five ranks based on its extent. Rank 1 was based on a combined ratio extent threshold of 50%, whereas for the other ranks the corresponding disparity normal distribution was used (68.3% for rank 2, 95.4% for rank 3, 99.7% for rank 4, and –100% for rank 5).

Based on the 42 SM observation points, the relationship between AVS30 (Average S wave velocity up to 30 m on the surface) and GH is shown in Fig. 12, and the relationship between AVS30 and GH rank is shown in Fig. 13. AVS30 is calculated from the PS logging results. Although a certain degree of disparity can be seen in the ranks for AVS30 and GH, generally they are correlated negatively. The correlation coefficient is 0.44 for AVS30-related GH, and at $R = 0.49$, the AVS30-related GH rank is slightly higher.

The GH rank and AVS30 (Fig. 14) were compared based on approximately 20 000 borehole data[15)]. The characteristics of the GH distribution (Figs. 12 and 13) are clearly portrayed in area A, where the GH rank is large by rivers where AVS30 is small, and in area D, where AVS30 is large and the GH rank is small. Furthermore, although it is difficult to evaluate the correlation using Tm and Rm alone, a strong correlation with GH can be seen in area B (where AVS30 is fairly large and GH is small) and area C (where AVS30 is fairly small and GH is fairly large).
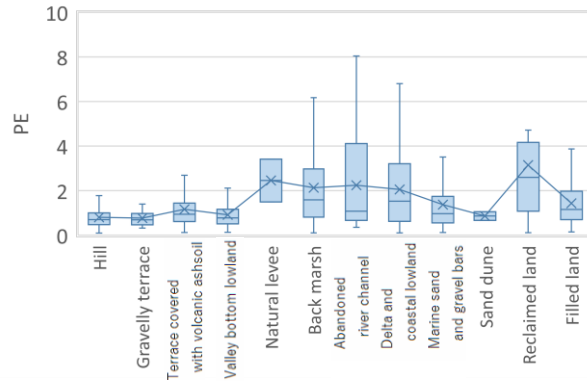
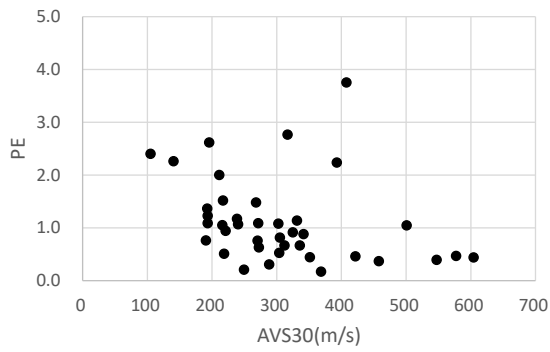Fig. 11 Disparity in ground hazard (GH) by geomorphology

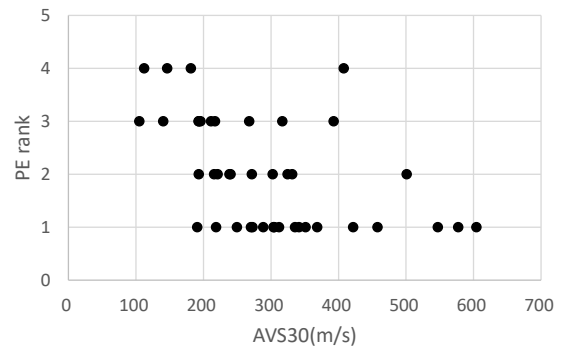Fig. 12 SM observation points, GH, and AVS30

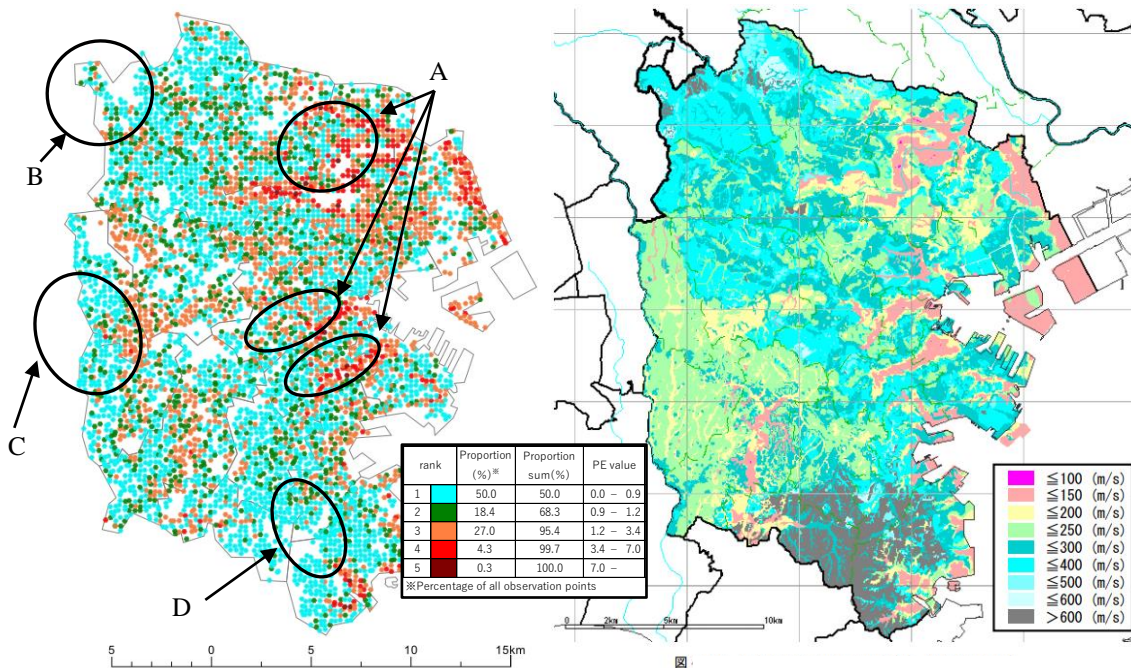Fig. 13 SM observation points, GH rank, and AVS30

rank	Proportion (%)※	Proportion sum(%)	PE value
1	50.0	50.0	0.0 – 0.9
2	18.4	68.3	0.9 – 1.2
3	27.0	95.4	1.2 – 3.4
4	4.3	99.7	3.4 – 7.0
5	0.3	100.0	7.0 –

※Percentage of all observation points

≦100 (m/s)	
≦150 (m/s)	
≦200 (m/s)	
≦250 (m/s)	
≦300 (m/s)	
≦400 (m/s)	
≦500 (m/s)	
≦600 (m/s)	
＞600 (m/s)	

Fig. 14 GH distribution (left) and AVS30 distribution using borehole data in Yokohama (right)

6. SUMMARY

We calculated the HVSR from MT records at approximately 5700 observation points in Yokohama and extracted the predominant period and peak values. We compared these to SM observation records of predominant period and peak values. We found that the predominant period matched at approximately 70% of points at which peaks were confirmed. The peak values supported the same trends.

To evaluate GH simply while considering only the MT results, we calculated the GH as the MT predominant period multiplied by the peak value, and we then compared this with AVS30 obtained from borehole data. There was disparity in the GH based on geomorphology, but it was confirmed to be consistent with the AVS30 distribution.

Henceforth, by performing a theoretical investigation using a simple model, we aim to confirm basic GH characteristics obtained by multiplying the predominant period by the peak value to investigate lowland topographical disparity factors and to develop a GH evaluation method that considers disparity. We also intend to investigate the applicability to regions other than Yokohama that have a greater density of seismic motions.

REFERENCES

1) Nakamura, Y.: A method for dynamic characteristics estimation of subsurface using microtremor on the ground surface, *Quarterly Report of RTRI*, Vol. 30, No. 1, pp. 25–33, 1989.
2) Tokimatsu, K. and Tamura, S.: Contribution of Rayleigh and body waves to displacement induced by a vertical point force on a layered elastic half-space, *Journal of Structural and Construction Engineering, Architectural Institute of Japan*, No. 476, pp. 95–101, 1995. (in Japanese)
3) Matsushima, S., Hirokawa, T., De Martin, F., Kawase, H. and Sanchez-Sesma, F. J.: The Effect of Lateral Heterogeneity on Horizontal-to-Vertical Spectral Ratio of Microtremors Inferred from Observation and Synthetics, *Bulletin of Seismological Society of America*, Vol. 104, No. 1, pp. 381–393, 2014.
4) Motoki, K., Watanabe, T., Kato, K., Takesue, K., Yamanaka, K., Iiba, M. and Koyama, S.: Characteristics of temporal and spatial variation in peak periods of horizontal to vertical spectral ratios of microtremors –Case study at flat engineering bedrock sites and its interpretation–, *Journal of Structural and Construction Engineering, Architectural Institute of Japan*, Vol. 81 No. 721, pp. 437–445, 2016. (in Japanese)
5) Nakamura, Y., Hara, T. and Yamada, M.: Study on risk evaluation method for ground shaking hazard by microtremor observation, *Journal of Japan Society of Civil Engineers, Ser. A1*, Vol. 74, No. 4, pp. 675–685, 2018. (in Japanese)
6) Ochiai, T., Yamamoto, T., Hattori, H. and Enomoto, T.: Study on zoning for ground shaking characteristics of surface soil structure in Sagami plain using spatially dense microtremor measurements, *Journal of Social Safety Science*, No. 5, pp. 21–26, 2003. (in Japanese)
7) Ueno, N., Enomoto, T. and Yamamoto, T.: Investigation of illustration and its characteristics for spatial distribution of predominant periods obtained from high density microtremor observations

in Yokohama City by using GIS., *The 13th Japan Earthquake Engineering Symposium*, GO31-Fri-PM-3, pp. 2011–2018, 2010. (in Japanese)

8) Yokohama Environmental Research Institute: Yokohama City topographic geological map, 2004.

9) Wakamatsu, K., Matsuoka, M., Kubo, S., Hasegawa, K. and Sugiura, M.: Development of GIS-based Japan engineering geomorphologic classification map, *Journal of Japan Society of Civil Engineers*, No. 759/I-67, pp. 213–232, 2004. (in Japanese)

10) Statistics Bureau, Ministry of Internal Affairs and Communications: *About Regional Mesh Statistics*, http://www.stat.go.jp/data/mesh/m_tuite.htm. (in Japanese, last accessed on May 29, 2019)

11) General Affairs Bureau, City of Yokohama: *Strong Motion Network*, http://www.city.yokohama.lg.jp/somu/org/kikikanri/eq/. (in Japanese, last accessed on May 29, 2019)

12) Toshinawa, T., Nishida, H., Midorikawa, S. and Abe, S.: Comparison between spectral characteristics evaluated from strong motions and microtremors at strong-motion sites in Yokohama, *Journal of Japan Society of Civil Engineers*, No. 640/I-50, pp. 193–202, 2000. (in Japanese)

13) Enomoto, T., Ishii, T., Yamamoto, T. and Sugimoto, M.: Comparative study of H/V spectrum characteristics between microtremor and seismic motion records, *Summaries of Technical Papers of Annual Meeting,* Architectural Institute of Japan (Kanto), Vol. B-2, pp. 87–88, 2006. (in Japanese)

14) Cabinet Office (Disaster Prevention): Technical data for creating an earthquake disaster prevention map, 2005. (in Japanese)

15) General Affairs Bureau, City of Yokohama: *Yokohama City Earthquake Damage Assumption Survey Report*, 2012. (in Japanese)

16) Bureau of Urban Development, Tokyo Metropolitan Government: *Your Community's Earthquake Risk 2018 The Eighth Community Earthquake Risk Assessment Study,* https://www.toshiseibi.metro.tokyo.lg.jp/bosai/chousa_6/download/earthquake_risk.pdf. (last accessed on June 22, 2020)